THE JOURNAL OF BIOLOGICAL CHEMISTRY VOL. 284, NO. 35, pp. 23818–23829, August 28, 2009

pH-dependent Internalization of Muramyl Peptides from Early Endosomes Enables Nod1 and Nod2 Signaling*

Received for publication, June 15, 2009 Published, JBC Papers in Press, July 1, 2009, DOI 10.1074/jbc.M109.033670

Jooeun Lee[‡], Ivan Tattoli[‡§], Kacper A. Wojtal[¶], Stephan R. Vavricka[¶], Dana J. Philpott[§], and Stephen E. Girardin[‡1]

From the [‡]Department of Laboratory Medicine and Pathobiology and [§]Department of Immunology, Medical Sciences Building, University of Toronto, 1 King's College Circle, Toronto, Ontario M5S 1A8, Canada and the [¶]Division of Gastroenterology and Hepatology, University Hospital Raemistrasse, 100 CH-8091 Zurich, Switzerland

Nod1 and Nod2 are members of the Nod-like receptor family that detect intracellular bacterial peptidoglycan-derived muramyl peptides. The biological effects of muramyl peptides have been described for over three decades, but the mechanism underlying their internalization to the cytosol remains unclear. Using the human epithelial cell line HEK293T as a model system, we demonstrate here that Nod1-activating ligands entered cells through endocytosis, most likely by the clathrin-coated pit pathway, as internalization was dynamin-dependent but not inhibited by methyl-β-cyclodextrin. In the endocytic pathway, the cytosolic internalization of Nod1 ligands was pH-dependent, occurred prior to the acidification mediated by the vacuolar ATPase, and was optimal at pH ranging from 5.5 to 6. Similarly, the Nod2 ligand MDP was internalized into host cytosol through a similar pathway with optimal pH for internalization ranging from 5.5 to 6.5. Moreover, Nod1-activating muramyl peptides likely required processing by endosomal enzymes, prior to transport into the cytosol, suggesting the existence of a sterically gated endosomal transporter for Nod1 ligands. In support for this, we identified a role for SLC15A4, an oligopeptide transporter expressed in early endosomes, in Nod1-dependent NF-κB signaling. Interestingly, SLC15A4 expression was also up-regulated in colonic biopsies from patients with inflammatory bowel disease, a disorder associated with mutations in *Nod1* and *Nod2*. Together, our results shed light on the mechanisms by which muramyl peptides get access to the host cytosol, where they are detected by Nod1 and Nod2, and might have implications for the understanding of human diseases, such as inflammatory bowel disease.

Innate immunity relies on the detection of conserved microbial- or danger-associated molecular patterns (MAMPs or DAMPs),[2] by pattern-recognition molecules. In mammals, several families of pattern-recognition molecules have been recently identified, including the transmembrane Toll-like receptors (TLRs), cytosolic Nod-like receptors (NLRs), and RIG-I-like receptors (1). NLR proteins include Nod1 and Nod2, which trigger pro-inflammatory pathways such as NF-κB and mitogen-activated protein kinases, in response to bacterial peptidoglycan (2), and NLRPs (also known as Nalps), such as NLRP1 and NLRP3, which induce the activation of caspase-1 inflammasomes in response to various MAMPs and DAMPs (3).

In the case of TLRs, there is accumulating evidence that the subcellular localization and the function of these pattern-recognition molecules is tightly associated, at multiple levels, with endocytosis and phagocytosis, which represent evolutionary conserved mechanisms for the internalization of small (<0.5 μm) and large (>0.5 μm) particles, respectively. Indeed, whereas some TLRs are expressed at the plasma membrane, others (such as TLR3, -7, and -9) are found predominantly associated with the endoplasmic reticulum and endosomal compartments, where they detect their respective microbial-derived nucleic acid MAMPs (4). In particular, TLR9 has been shown to move from the endoplasmic reticulum to CpG DNA-containing endosomes, concurrent with the accumulation of MyD88, thus showing that endosomes represent the physiological location where TLR9-dependent signaling arises (5). In addition, studies on TLR4 have demonstrated that lipopolysaccharide (LPS) is endocytosed by a receptor-mediated mechanism dependent on dynamin and clathrin and co-localized with TLR4 on early/sorting endosomes (6). In the case of this TLR, it is believed that endosomal trafficking is associated with termination of the MyD88-dependent pro-inflammatory signal (6). In contrast, TLR4 in early endosomes has been shown recently to engage TRAM and TRIF adaptors, resulting in the ignition of type I interferon signaling in response to LPS (7). Therefore, the nature of the cellular response to LPS is dependent upon the subcellular localization of TLR4, thus reinforcing the importance of the interplay between TLR signaling and endosomal trafficking.

A number of studies have also linked TLR signaling with phagosome maturation. Although it remains controversial whether TLR-dependent signaling actually drives phagosomal

* This work was supported by grants from Canadian Institutes of Health Research (to D. J. P.), Crohn's and Colitis Foundation of Canada (to S. E. G.), and the Sandler Program for Asthma Research (to D. J. P.). This work was also supported by the Swiss National Science Foundation (Grant 320000-114009/1 to S. R. V. and K. A. W.), Grant 3347CO-108792 (Swiss IBD Cohort), and a grant of the Zurich Center of Integrative Human Physiology.

[1] To whom correspondence should be addressed: Medical Sciences Bldg., Rm. 6336, University of Toronto, Toronto, Ontario M5S 1A8, Canada. Tel.: 416-978-7507; Fax: 416-978-5959; E-mail: Stephen.girardin@utoronto.ca.

[2] The abbreviations used are: MAMP, microbial-associated molecular patterns; DAMP, danger-associated molecular pattern; TLR, Toll-like receptor; NLR, Nod-like receptor; LPS, lipopolysaccharide; MDP, muramyl dipeptide; DAP, diaminopimelic acid; M-Tri-DAP, *N*-acetylmuramyl-L-Ala-D-Glu-*meso*DAP; iE-DAP, dipeptide D-Glu-*meso*DAP; IBD, inflammatory bowel disease; V-ATPase, vascular ATPase; DMEM, Dulbecco's modified Eagle's medium; siRNA, small interference RNA; MβCD, methyl-β-cyclodextrin; SLC, solute carrier; IB, isotonic buffer; CD, Crohn's disease; UC, ulcerative colitis.

maturation (8, 9), it is clear that the processing of engulfed microbes within phagosomes regulates the availability of MAMPs within this compartment. Accordingly, Herskovits *et al.* have recently demonstrated that, in interferon Γ-activated macrophages, the degradation of *Listeria monocytogenes* in the phagolysosome generates bacterial molecules, which could specifically trigger type I interferon responses through a Nod2-dependent pathway (10). This interesting observation suggests that innate immune signaling and microbial degradation within the phagolysosome are processes that are intimately linked. It also provides support to the concept that Nod-dependent signaling is associated with intracellular vesicular trafficking.

Nod1 and Nod2 both detect specific structures from bacterial peptidoglycan (11). Whereas Nod2 detects muramyl dipeptide (MDP) (12, 13), a motif found in almost all bacteria, Nod1 specifically senses diaminopimelic acid (DAP)-containing muramyl peptides (14, 15). In particular, human Nod1 preferentially detects *N*-acetylmuramyl-L-Ala-D-Glu-*meso*DAP (M-Tri-DAP) (16), and the minimal motif for Nod1-dependent sensing is the dipeptide D-Glu-*meso*DAP (iE-DAP) (11, 14). Interestingly, long before the identification of Nod1 and Nod2 as sensors of muramyl peptides and bacterial peptidoglycan, the biological activities of these bacterial-derived molecules had been studied extensively (17, 18). It is well documented that these muramyl peptides trigger a multitude of immune responses, such as the induction of cytokines/chemokines, the production of nitric oxide and reactive oxygen species, and the clearance of microbes by phagocytic cells (17, 18). A considerable literature also demonstrated that these muramyl peptides synergize with MAMPs detected by TLRs, such as LPS (19). Although the identification of Nod1 and Nod2 as sensors of muramyl peptides has provided an acceleration in this field of investigation, it also brought the question of how such microbial molecules could get access to the host cytosol, where Nod1 and Nod2 reside. Interestingly, research aiming at improving the biological activities of these muramyl peptides demonstrated early on that the addition of lipophilic groups to these molecules enhanced their activity considerably, suggesting that their internalization was likely a key factor in determining their efficiency (20–23).

The mechanisms by which muramyl peptides get access to the host cytosol remain unclear. This question is of fundamental importance for our understanding of Nod-dependent signaling and potentially holds broad therapeutic implications. Indeed, mutations in *Nod1* and *Nod2* have been associated with inflammatory bowel disease (IBD) in humans (24). In particular, *Nod2* has been identified as the first susceptibility gene for Crohn's disease (25, 26).

In this report, we used the HEK293T epithelial cell line to study the mechanism of internalization of Nod1 ligands. We demonstrated that these peptidoglycan-derived molecules enter cells by endocytosis, and that the composition of the Nod1-activating molecules dramatically affected their intrinsic uptake capacity. Our data also suggested that this internalization was mediated by clathrin-dependent endocytosis, because internalization of Nod1 ligands required dynamin and was independent from caveolae. Further, we showed that, within endosomes, the internalization of Nod1 ligands was critically dependent on pH, and was optimal at pH ranging from 5.5 to 6, which are characteristic of early endosomes. Accordingly, internalization of Nod1-activating molecules did not require the action of the vacuolar ATPase (V-ATPase) complex. We also provide evidence that the Nod2 ligand MDP enters cells through a similar endocytic process. Our results also show that the internalization of Nod1 ligands is a process that is sterically gated, and likely requires the action of hydrolytic endosomal enzymes prior to transport into the cytosol, thus suggesting the existence of one or several specific transporters for Nod1 ligands in early endosomes. Using knockdown assays, we identified SLC15A4 as a putative transporter for Nod1 ligands in early endosomes. SLC15A4 expression was found to be significantly up-regulated in tissue biopsies from IBD patients, therefore highlighting a potential role for the modulation of peptidoglycan access to the cytosol in IBD etiology. Together, our results uncover the mechanism by which Nod ligands traffic into cells and get access to the cytosol where they are detected by Nod1 and Nod2. Our observations also highlight the previously unappreciated link between endosomal acidification/maturation and Nod-dependent signaling.

EXPERIMENTAL PROCEDURES

Cell Culture and Reagents—Human embryonic kidney epithelial cell line HEK293T (American Type Culture Collection) was cultured in Dulbecco's modified Eagle's medium (DMEM), supplemented with 5% fetal calf serum, and 1% penicillin/streptomycin. Cells were maintained in 95% air, 5% CO_2 at 37 °C. Endotoxin-free fetal calf serum and phosphate-buffered saline were from Wisent (St-Bruno, Quebec). Fetal calf serum was used after heat inactivation at 56 °C for 30 min. All cell culture reagents and antibiotics were also from Wisent.

Nod1 ligands, iE-DAP (γ-D-Glu-*meso*DAP), Tri-DAP (L-Ala-D-Glu-*meso*DAP), M-Tri-DAP (MurNAc-L-Ala-D-Glu-*meso*-DAP), C12-iE-DAP, were from InvivoGen. iE-DAP, Tri-DAP, and M-Tri-DAP were used at concentrations ranging from 1 to 10 μg/ml, whereas C12-iE-DAP was used from 0.01 to 1 μg/ml. Nod2 ligand, MDP was also from InvivoGen and used at a concentration of 10 μg/ml.

The inhibitors of endocytosis were purchased from Sigma and used at the following concentrations: valinomycin (1–10 μM), bafilomycin A1 (10–50 nM), Dynasore monohydrate (80 μM), nocodazole (1 μg/ml), cytochalasin D (1 μg/ml), carbonyl cyanide *m*-chlorophenylhydrazone (1–10 μM), and methyl-β-cyclodextrin (2.5–10 mM).

Extracellular Acidification Assays—To examine the effect of extracellular pH on ligand uptake, isotonic buffer (IB) (50 mM HEPES, pH 7, 100 mM KCl, 3 mM $MgCl_2$, 0.1 mM dithiothreitol, 85 mM sucrose, 0.2% bovine serum albumin, 1 mM ATP, and 0.1 mM GTP) was prepared with pH modified to 5, 5.5, 6, 6.5, or 7, and ATP, dithiothreitol, and GTP were added freshly for each experiment. Cells were then incubated for 1 h at 37 °C with the respective ligands in 500 μl of IB at varying pH. Subsequently, IB was removed and replaced with DMEM plus 5% fetal-calf serum for 5 h before performing luciferase measurements.

NF-κB Activation Assays—Transfections were carried out using polyethylenimine (Polysciences Inc., Warrington, PA) in HEK293T according to the manufacturer's instructions.

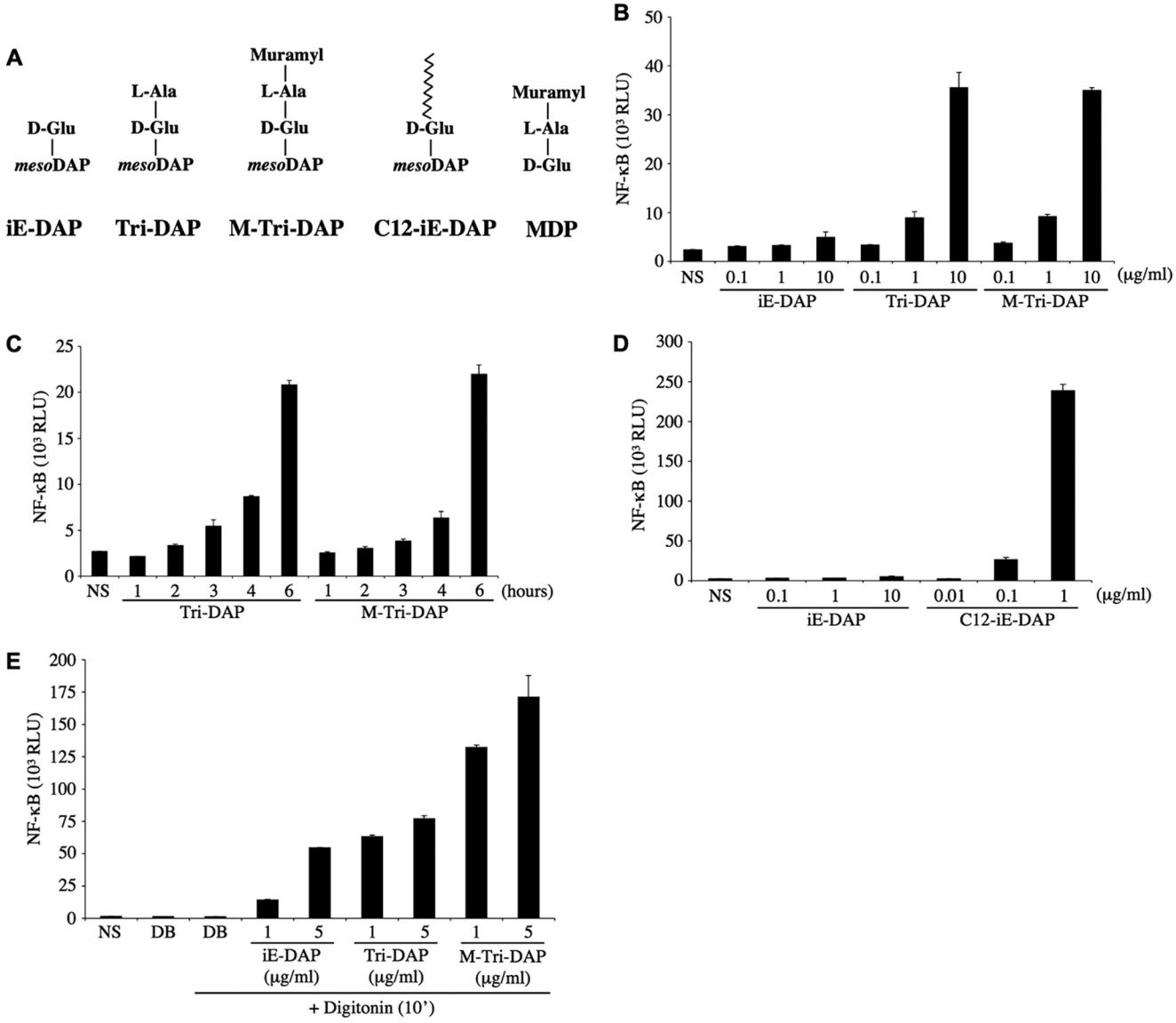

FIGURE 1. **Differential entry of Nod1 ligands into HEK293T cells.** *A*, Nod1- and Nod2-activating molecules used in this study. The four Nod1-activating molecules contain the minimal motif D-Glu-*meso*DAP (iE-DAP) that triggers Nod1. C12-iE-DAP contains a fatty acid moiety (lauroyl group) linked to the D-Glu. MDP stimulates Nod2 activity. All these molecules are synthetic and therefore do not contain any microbial contaminant. *B*, HEK293T cells were transfected overnight with the NF-κB reporter plasmid Igκ-luci. The following day, increasing concentrations of Nod1 ligands iE-DAP, Tri-DAP, or M-Tri-DAP were added to the cell culture medium for 6 h before cell lysis. *C*, HEK293T cells were transfected with Igκ-luci overnight and Tri-DAP or M-Tri-DAP were added to the cell culture medium for 1–6 h on the following day, as indicated. *D*, same as *B*, but comparing the responses to increasing concentrations of iE-DAP and C12-iE-DAP. *E*, HEK293T cells were transfected overnight with Igκ-luci in DMEM cell culture medium. The following day, cell culture medium was replaced to an isotonic digitonin buffer (*DB*) and iE-DAP, Tri-DAP, or M-Tri-DAP (all at either 1 μg/ml or 5 μg/ml) were added to the cells in the presence of digitonin for 10 min. Then, cell culture medium was replaced to DMEM for 6 h, before cell lysis. *NS*, non-stimulated.

Briefly, cells were transfected overnight with 75 ng of NF-κB luciferase reporter plasmid (Igκ-luc, Invitrogen). The empty vector (pcDNA3.1, Invitrogen) was used to balance the transfected DNA concentration. The expression vector for human Nod2 (0.2 ng/well) was a kind gift from Dr. G. Nunez (University of Michigan, Ann Arbor, MI). Following transfection, Nod1 or Nod2 ligands were added the next day for 6 h (unless specified) before performing luciferase measurements. For NF-κB activation assays in digitonin-permeabilized cells, HEK293T were incubated for 10 min at 37 °C with Nod1 ligands in isotonic digitonin buffer (DB) (500 μl) with or without 10 μg/ml digitonin (Sigma), and then placed in DMEM for 6 h, as previously described (15).

As a control for the possible toxicity of the trafficking inhibitors used toward NF-κB activation, we systematically transfected overnight the Igκ-luci reporter vector together with 50 ng of expression vector encoding for Rip2 (from Dr. M. Thome, Université de Lausanne, Lausanne), the Nod1 adaptor protein acting downstream of the detection of peptidoglycan by Nod1. In all the experiments presented in this study, the doses of the drugs used had no effect on Rip2-mediated activation of NF-κB (data not shown). NF-κB-dependent luciferase assays were performed in duplicate, and data represent at least three independent experiments. Data show mean ± S.E.

Immunofluorescence—HEK293T cells were incubated in DMEM without fetal calf serum for 1 h prior to incubation in IB

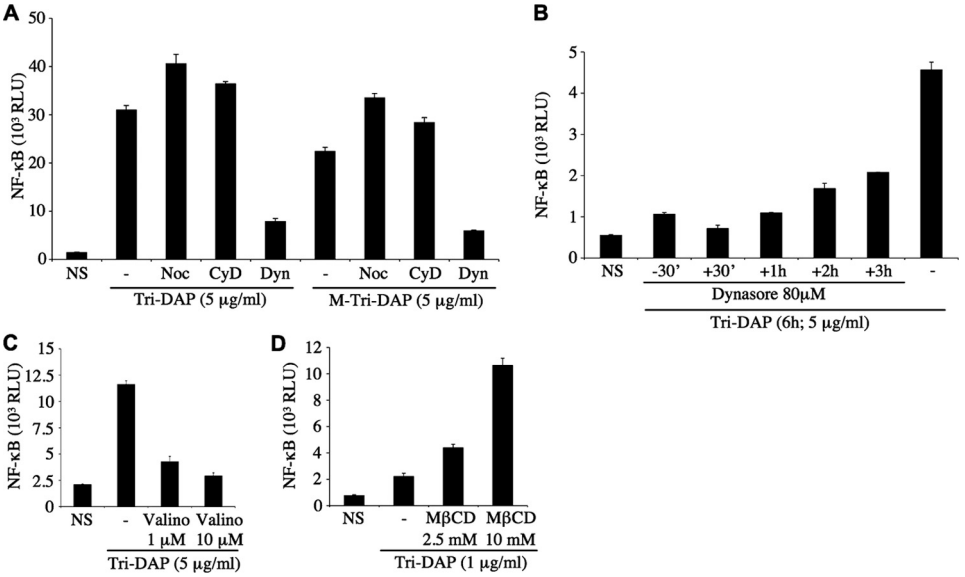

FIGURE 2. **Nod1 ligands enter HEK293T cells by endocytosis.** In all experiments below, HEK293T cells were first transfected overnight with Igκ-luci. *A*, cells were stimulated for 6 h with 5 μg/ml Tri-DAP or M-Tri-DAP in the absence or presence of the cellular trafficking inhibitors nocodazole (*Noc*, 1 μg/ml), cytochalasin D (*CyD*, 1 μg/ml), and Dynasore (*Dyn*, 80 μM). *B*, cells were stimulated for 6 h with 5 μg/ml Tri-DAP, in the presence or absence of Dynasore (80 μM) added either prior to the Nod1 ligand (−30′), or at various times after the addition of Tri-DAP, as indicated. *C*, cells were stimulated for 6 h with 5 μg/ml Tri-DAP in the absence or presence of valinomycin (*Valino*, 1 μM or 10 μM). *D*, cells were stimulated for 6 h with 1 μg/ml Tri-DAP in the absence or presence of methyl-β-cyclodextrin (*MβCD*, 2.5 mM or 10 mM). *NS*, non-stimulated.

at pH 5.5 or 7 plus transferrin conjugated to Alexa Fluor 568 (10 μg/ml, Molecular Probes Inc.) for 1 h at 37 °C. Rab5-RFP expression vector was a kind gift from Dr. John Brumell (the Hospital for Sick Children, Toronto). SLC15A4-V5 was obtained from Dr. Knipp (The State University of New Jersey). Cells were co-transfected with either Rab5-RFP (500 ng) or SLC15A4-V5 (500 ng) or both overnight, and incubated in IB at pH 5.5 or 7 for 1 h at 37 °C the next day. Cells were then washed with cold phosphate-buffered saline, fixed for 15 min at room temperature with paraformaldehyde (3.7% w/v in phosphate-buffered saline), permeabilized with 0.1% Triton X-100 for 5 min, stained with anti-V5 (anti-mouse-fluorescein isothiocyanate) for 1 h, and mounted with Vectashield (Vector Laboratories, Burlingame, CA). Coverslips were visualized on a Carl Zeiss Axiovert 200M microscope with a 63× oil fluorescence objective.

Semi-quantitative PCR—Total RNA samples from untreated cells were prepared according to the manufacturer's protocols (Qiagen). After genomic DNA elimination with RNase-free DNase, the complementary DNA was generated from 1 μg of RNA using a mixture of oligo(dT) and random primers and Omniscript Reverse Transcriptase (Qiagen). PCR was performed with *Taq* polymerase (Invitrogen) using the following primers: 5′-TTGCTTCTGGTCGTCTGTG-3′ and 5′-GCCCCTGACATGAAATATGG-3′ for SLC15A1, 5′-GCCCTGTCTTGAAGCATTTT-3′ and 5′-AGAGTCTCTGGGGCCTTGTT-3′ for SLC15A2, 5′-GCTTAAGCTCGCTCTCCAAA-3′ and 5′-GCAAGATCTTCACCAGCAC-3′ for SLC15A3, and 5′-AGCGATCCTGTCGTTAGGTG-3′ and 5′-AGGAGGCTTGGTGATGAAAA-3′ for SLC15A4.

Design and Construction of siRNA Sequences against Human SLC15A4—The sequences of the siRNA specifically targeting *SLC15A4* gene were purchased from Ambion (Silencer Predesigned siRNA) siRNA ID # S42440 and siRNA ID #S42441 or designed through siRNA Wizard v3.0 (InvivoGen). The sequences were the following: 5′-CGGCTGCTATTTGAACTAT-3′ for #B, 5′-GCAGACAACATATGTTTTA-3′ for #A, 5′-GAGTCTTTCAGCAATCTTCTA-3′ for #C, 5′-GATTCATGTAAGATGTCTCAT-3′ for #D, 5′-GTGGAGAGCGCCAGAGTAA-3′ for #E, 5′-GATTCATGTAAGATGTCTCAT-3′ for #F, and 5′-CGGCTGCTATTTGAACTAT-3′ for scrambled. Two different vectors were used to generate shRNA against SLC15A4; pLKO.1 vector (Addgene, Cambridge, MA) for lentiviral knockdown system, and psiRNA-h7SK-GFPzeo transient knockdown of SLC15A4 expression. For both vectors, positive clones were identified by restriction digestion and confirmed by sequencing.

Lentiviral Vector Cloning—The sense and antisense oligonucleotides were resuspended in water at 20 μM and annealed by incubating at 95 °C for 4 min, 70 °C for 10 min, then decreasing the temperature to room temperature slowly (0.1 °C/min). The resulting lentiviral shRNA vector was confirmed by restriction enzyme digestion with AgeI/EcoRI. The constructed vector was also confirmed by DNA sequencing with pLKO.1 sequencing primer (5′-CAAGGCTGTTAGAGAGATAATTGGA-3′).

Lentivirus Packaging—Packaging and purification of the lentivirus were performed according to classic procedures. Briefly, HEK293T cells were seeded 1.5×10^6 in a 10-cm culture dish, in DMEM supplemented with 10% fetal bovine serum without antibiotics. The following day, cells were co-transfected with the lentiviral vector (1 μg), and the lentiviral packaging/envelope vectors psPAX2 (750 ng) and pMD2.G (250 ng). Viruses were collected from the culture supernatant 48 h post-transfection and spun at 1250 rpm for 5 min, and the media were passed through a 0.45-μm filter.

Lentiviral Transduction in HEK293T Cells—Cells were seeded in either 6-well plates or 24-well plates, and then incubated with lentivirus for 3 days. Polybrene (10 μg/ml) was added to increase the efficiency of lentiviral transduction. Following transduction, cells were co-transfected with NF-κB luciferase constructs, and luciferase assays were performed as above.

Western Blotting—HEK293T cells were centrifuged, and the pellet was lysed with radioimmune precipitation assay buffer (0.5 M Tris-HCl, pH 7.5, 150 mM NaCl, 1% Nonidet P-40, 0.5% deoxycholic acid, protease inhibitor mixture (Sigma P8340)). Total cell lysates were boiled for 10 min and subsequently subjected to SDS-PAGE. Western blot was performed according to a standard protocol, using a rabbit polyclonal anti-SLC15A4 (Santa Cruz Biotechnology, dilution 1:500), followed by incu-

bation with a secondary anti-rabbit horseradish peroxidase antibody (Thermo Scientific, 1:10,000) and an enhanced Chemiluminescence Kit (PerkinElmer Life Sciences). Mouse monoclonal anti-tubulin (Sigma, T9026, 1:10,000) was used as loading control.

SLC15A4 Expression in IBD Patients—The analysis of SLC15A4 expression in 49 CD patients and 53 UC patients was performed in the context of a larger study, which was reported elsewhere (36).

RESULTS

HEK293T cells transfected overnight with an expression vector encoding for luciferase under the control of an NF-κB-responsive promoter (Igκ-luci) were stimulated with increasing concentrations of the Nod1 ligands iE-DAP, Tri-DAP, or M-Tri-DAP for 6 h. iE-DAP represents the minimal peptide activating Nod1, whereas Tri-DAP is the minimal naturally occurring Nod1 ligand, and M-Tri-DAP is the minimal muramyl peptide stimulating Nod1 (11, 14) (Fig. 1*A*). Although Tri-DAP and M-Tri-DAP activated cells comparably, iE-DAP appeared to be a very poor agonist, even at the highest dose tested (10 μg/ml) (Fig. 1*B*). We next stimulated cells for 1–6 h with 10 μg/ml of Tri-DAP or M-Tri-DAP, and observed that these Nod1 ligands required at least 3–4 h of stimulation to induce measurable activation of the NF-κB reporter gene (Fig. 1*C*). We and others have previously demonstrated that iE-DAP is able to trigger Nod1-dependent NF-κB activation in a setting where the ligands were added overnight together with a liposomal transfection reagent (11, 14). Therefore, the results above likely reflect the fact that iE-DAP, contrary to Tri-DAP or M-Tri-DAP, is inefficiently internalized by HEK293T cells. To study this question further, we used a derivative iE-DAP that contains a lauroyl (C12) group attached to the glutamic residue of iE-DAP (see Fig. 1*A*). The rationale for such a modification is that the fatty acids may form micelle-like structures and display enhanced internalization. We observed that the addition of the fatty acid moiety to iE-DAP enhanced >100-fold the capacity of the Nod1 ligand to trigger NF-κB (Fig. 1*D*). This suggests that iE-DAP-activated cells poorly as a result of defective trafficking, rather than because of an intrinsic inefficiency to stimulate Nod1. Next, we questioned if the Nod1 ligands actually needed to get access to the host cytosol to trigger cellular responses, or if trafficking and targeting to a specific subcellular compartment were the only requirement for Nod1-dependent activation. To answer this question, we pulsed HEK293T cells with iE-DAP, Tri-DAP, or M-Tri-DAP for 10 min in the presence of digitonin, a membrane-permeabilizing toxin, then replaced back the cell culture medium to neutralize the action of digitonin, and lysed cells 6 h post-stimulation. Interestingly, in this experimental setting, all Nod1 ligands potently stimulated cells (Fig. 1*E*), therefore showing that presentation to the host cytosol is the limiting factor for their activating capacities. It must be noted, however, that, in this context, iE-DAP remained a weaker agonist than Tri-DAP or M-Tri-DAP (Fig. 1*E*), which correlates well with our previous observations using a different experimental setting (11), and may reflect a difference in the intrinsic capacity of this dipeptide to trigger Nod1, as compared with the naturally occurring tripeptide forms. Together, these

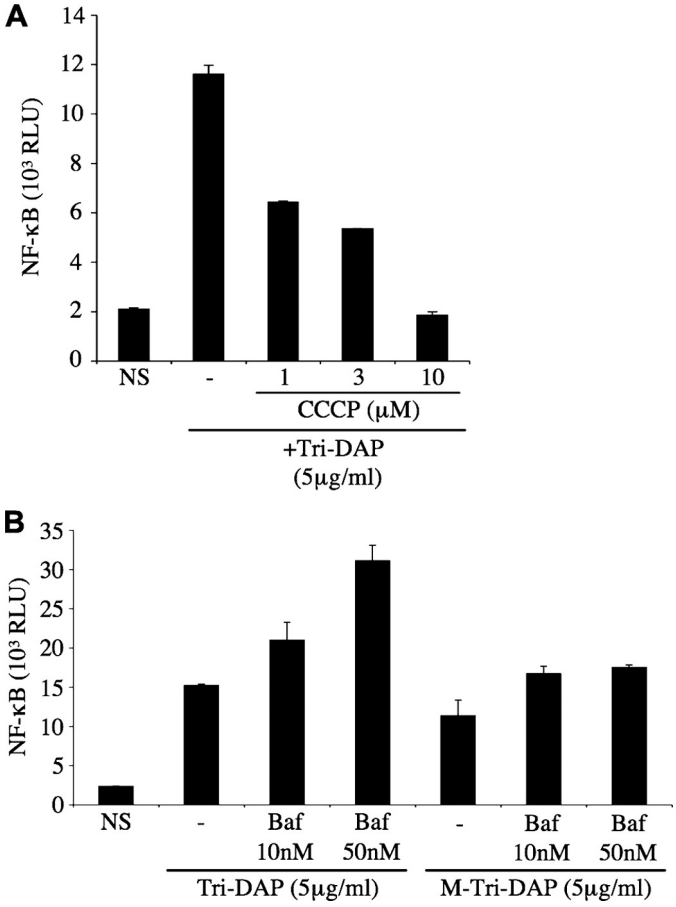

FIGURE 3. **The internalization of Nod1 ligands is dependent on endosomal pH.** In the experiments below, HEK293T cells were first transfected overnight with Igκ-luci. *A*, cells were stimulated for 6 h with 5 μg/ml Tri-DAP in the absence or presence of carbonyl cyanide *m*-chlorophenylhydrazone (*CCCP*, 1–10 μM). *B*, cells were stimulated for 6 h with 5 μg/ml Tri-DAP or M-Tri-DAP in the absence or presence of bafilomycin A1 (*Baf*, 10–50 nM). *NS*, non-stimulated.

results show that epithelial cells have the capacity to internalize Nod1 ligands and that these molecules display different trafficking abilities and demonstrate that these agonists must reach the host cytosol to trigger Nod1-dependent responses.

We next investigated the cellular pathways responsible for the internalization of Nod1 ligands into HEK293T cells. Nocodazole and cytochalasin D, two drugs that block macropinocytosis by disrupting microtubules and actin cytoskeleton, respectively, did not affect the capacity of Tri-DAP or M-Tri-DAP to stimulate cells (Fig. 2*A*). In contrast, Dynasore, a highly specific inhibitor of dynamin (27), potently blocked Tri-DAP- and M-Tri-DAP-dependent activation of NF-κB (Fig. 2*A*). We next took advantage of the fact that Dynasore blocks dynamin in seconds or minutes (27), to study further the kinetics of dynamin-dependent entry of Nod1 ligands into cells, by adding the drug at various times before or after the addition of Nod1 ligand. Using this technique, we observed that the endocytosis of Nod1 ligands is a slow and continuous process that occurs in a linear fashion over time (Fig. 2*B*). Because dynamin is known to be crucial for both clathrin-coated and caveolae vesicular endocytic pathways (28, 29), we aimed to distinguish between these two potential entry mechanisms. Intracellular potassium depletion specifically blocks clathrin-dependent endocytosis (28,

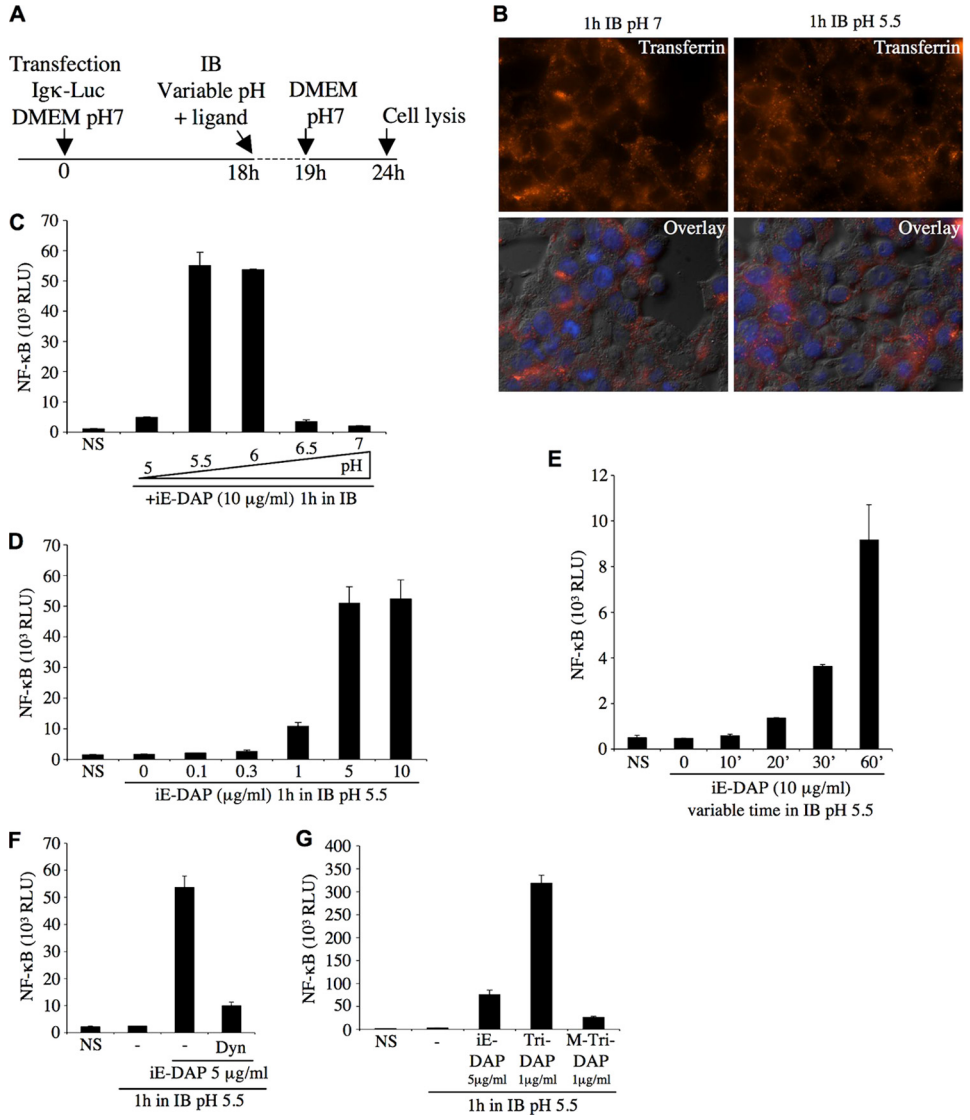

FIGURE 4. **Extracellular acidification strongly potentiates endocytosis-mediated entry of iE-DAP.** *A*, schematic representation of the experimental procedure followed to study the influence of extracellular pH on NF-κB activation by Nod1 ligand iE-DAP. The acidification was maintained for only 1 h, in a specific isotonic buffer (*IB*), a period when the ligand was added. Cell medium was replaced to DMEM, pH 7, for the last 5 h, before cell lysis. *B*, uptake of transferrin-Alexa Fluor 568 (10 μg/ml) by HEK293T cells for 1 h in IB buffer, pH 7 (*left*) or pH 5.5 (*right*), was followed by fluorescence microscopy. Overlay with differential interference contrast is also shown. For the experiments below (*C–G*), HEK293T cells were first transfected overnight with Igκ-luci, and transient acidosis in IB was performed, as described in *A*. *C*, cells were stimulated for 1 h with iE-DAP (10 μg/ml) in IB buffer at different pH, as indicated. *D*, cells were stimulated for 1 h with various concentrations of iE-DAP (0.1–10 μg/ml) in IB buffer, pH 5.5. *E*, cells were stimulated for various times (0–60 min) with iE-DAP (10 μg/ml) in IB buffer, pH 5.5. *F*, cells were stimulated for 1 h with iE-DAP (5 μg/ml) in IB buffer, pH 5.5, in the presence or absence of Dynasore (*Dyn*, 80 μM). *G*, cells were stimulated for 1 h with iE-DAP (5 μg/ml), Tri-DAP (1 μg/ml), or M-Tri-DAP (1 μg/ml) in IB buffer, pH 5.5. *NS*, non-stimulated.

29). Therefore, we dissipated K^+ gradients by treating cells with valinomycin, a K^+ ionophore, and observed that this drug potently blunted the cellular response to Nod1 ligands (Fig. 2*C*). Moreover, we used methyl-β-cyclodextrin (MβCD), a molecule that alters the fluidity of the plasma membrane by depleting cholesterol and known to perturb caveolae vesicular endocytic pathways (29). Strikingly, we observed that MβCD actually potentiated the cellular response to Nod1 ligands (Fig. 2*D*), thus excluding a role for caveolae in mediating the entry of Nod1 ligands into HEK293T cells. Together, these results identify clathrin-dependent endocytosis as the mode of entry of Nod1 ligands into HEK293T epithelial cells.

Endosomal maturation results in progressive acidification of the vesicular lumen, through a series of events, involving first the action of proteins such as the Na^+/H^+ exchangers, followed by further acidification mediated by the V-ATPase complex in late endosomes and lysosomes (30). We aimed to identify whether endosomal acidification played a role in the ability of Nod1 ligands to get exported to the cytosol. Cells treated with carbonyl cyanide *m*-chlorophenylhydrazone, an H^+ ionophore, displayed blunted responses to Nod1 ligands (Fig. 3*A*), thus suggesting that cellular proton gradients are critical for the trafficking and/or internalization of Nod1 ligands into host cytosol. Using bafilomycin A1, a specific inhibitor of V-ATPases, we observed that the acidification induced by this pump was not required for optimal trafficking of Nod1 ligands (Fig. 3*B*), therefore showing that these agonists likely exit the endocytic pathway in early/sorting endosomes. Of note, we noticed that bafilomycin A1 actually increased cellular responses to Nod1 ligands, which might be explained by the fact that early endosomes, stalled at a mildly acidified stage, are blocked at a pH close to the one optimal for transport of Nod1 ligands out of the endocytic machinery.

Our last results suggested that an optimal luminal pH might exist for the efficient transport of Nod1 ligands to the cytosol. To study this question further, we developed a procedure, relying on the transient (60 min) acidification of the extracellular milieu in an isotonic buffer in the presence of Nod1 ligands (Fig. 4*A*). Strikingly, we observed that, although this procedure did not affect clathrin-mediated endocytosis in general (Fig. 4*B*), it altered greatly the cellular response to the Nod1 ligand iE-DAP. In particular, we identified that an optimal pH for triggering Nod1-dependent responses existed and was around pH 5.5–6 (Fig. 4*C*), which is a level of acidification commonly observed in early endosomes (30). The fact that, through this experimental procedure, we could observe considerable cellular activation by iE-DAP reinforces the idea that this ligand is not intrinsically a poor Nod1 ligand but, rather, is impaired in its capacity to reach endosomes acidified to 5.5–6. Through titration (Fig. 4*D*) and kinetics (Fig. 4*E*) experiments, we refined our observations and

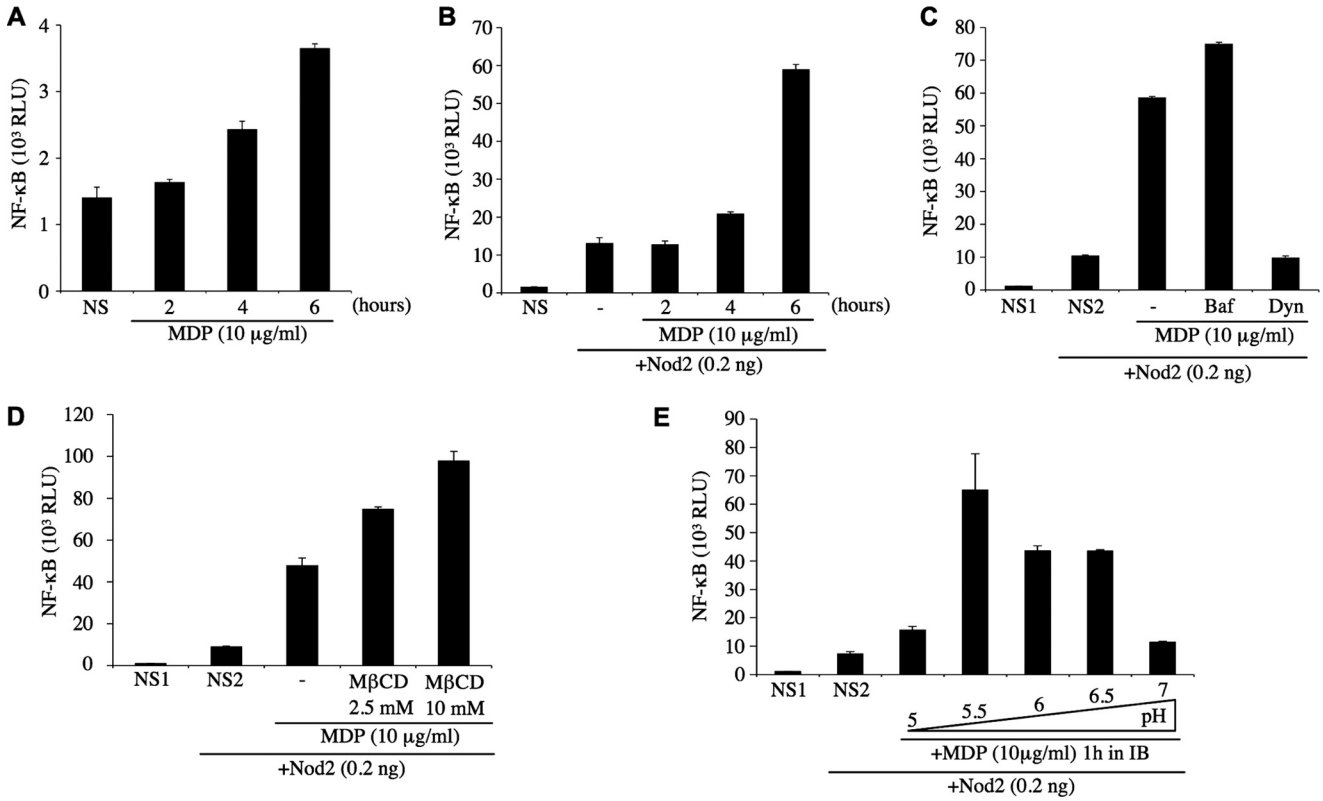

FIGURE 5. **The Nod2 ligand MDP enters HEK293T cells by endocytosis.** In all experiments below, HEK293T cells were first transfected overnight with Igκ-luci. *A*, cells were stimulated for various times (2–6 h) with muramyl dipeptide (*MDP*, 10 μg/ml). For the next experiments (*B–E*), cells were co-transfected with an expression vector encoding for hNod2 (0.2 ng/well). *B*, cells were stimulated for various times (2–6 h) with MDP (10 μg/ml). *C* and *D*, cells were stimulated for 6 h with MDP (10 μg/ml) in the presence or absence of bafilomycin A1 (*Baf*, 50 nM), Dynasore (*Dyn*, 80 μM) (*C*) or MβCD (2.5 mM or 10 mM) (D). *E*, cells were stimulated for 1 h with MDP (10 μg/ml) in IB buffer at different pH, similarly to Fig. 4*C*. *NS1*, non-stimulated; *NS2*, non-stimulated but overexpressing hNod2 (0.2 ng/well).

noticed that as little as 1 μg/ml of iE-DAP, and a transient extracellular acidosis for 20 min or more, induced measurable iE-DAP-dependent cellular responses. More importantly, we demonstrated that the procedure of transient extracellular acidosis that we developed likely bypassed normal endosomal maturation, but still relied on dynamin-dependent pinching off of endosomes from the plasma membrane, as it was fully blocked by Dynasore (Fig. 4*F*). Next, we used this procedure of transient extracellular acidosis to compare the relative capacities of distinct Nod1 ligands to trigger cellular NF-κB responses. We first noticed that the tripeptide ligand Tri-DAP displayed more potent activating capacities than iE-DAP (Fig. 4*G*), in agreement with our previous experiments using different experimental systems (see above). Surprisingly, we observed in this experimental setting that M-Tri-DAP was almost completely unable to trigger cellular responses (Fig. 4*G*), whereas M-Tri-DAP and Tri-DAP displayed similar activating capacities in normal stimulating conditions (see Fig. 1*B*). These results suggest that a processing of M-Tri-DAP into Tri-DAP likely occurs in normally maturing endosomes, which is bypassed in our experimental system where endosomal acidification is artificially provoked by transient acidosis (see also below Fig. 9). These observations also provide evidence that the exit of Nod1 ligands from early endosomes is a process that is sterically gated, thus indirectly suggesting the existence of a specific transport system for Nod1 ligands within the early endosome.

We then aimed to identify if the internalization of the Nod2 ligand, MDP, displayed similar characteristics than that of Nod1 ligands in HEK293T cells. When added extracellularly for 2–6 h, we observed that MDP triggered only minimal NF-κB-dependent cellular responses (Fig. 5*A*), which is in agreement with previous reports on Nod2-dependent responses in epithelial cells (15). Indeed, it has been reported by several groups that the levels of Nod2 expression in most epithelial cells, including HEK293T, is minimal or absent in normal conditions (31, 32). Therefore, we co-transfected overnight minimal amounts of a Nod2-expressing vector (0.2 ng) together with our Igκ-luci reporter construct, and then stimulated cells with MDP for increasing periods the following day. Using this procedure, we noticed an increase in the overall sensitivity of HEK293T cells to MDP (Fig. 5*B*), which prompted to select this experimental setting for further studies. Next, we observed that MDP, like Nod1 ligands, entered cells through dynamin-dependent and caveosome-independent endocytosis (Fig. 5, *C* and *D*), and that the export out of the endocytic machinery occurred prior to acidification dependent on the action of the V-ATPase, as it was not blocked by bafilomycin A1 (Fig. 5*C*). Finally, using the transient extracellular acidosis procedure described above, we observed that MDP internalization also required an optimal pH in HEK293T cells, but that it exhibited a broader range of pH 5.5 to 6.5 (Fig. 5*E*) than that of Nod1 ligands.

Next, we aimed to identify the nature of the putative transporter, expressed in early endosomes, which was responsible

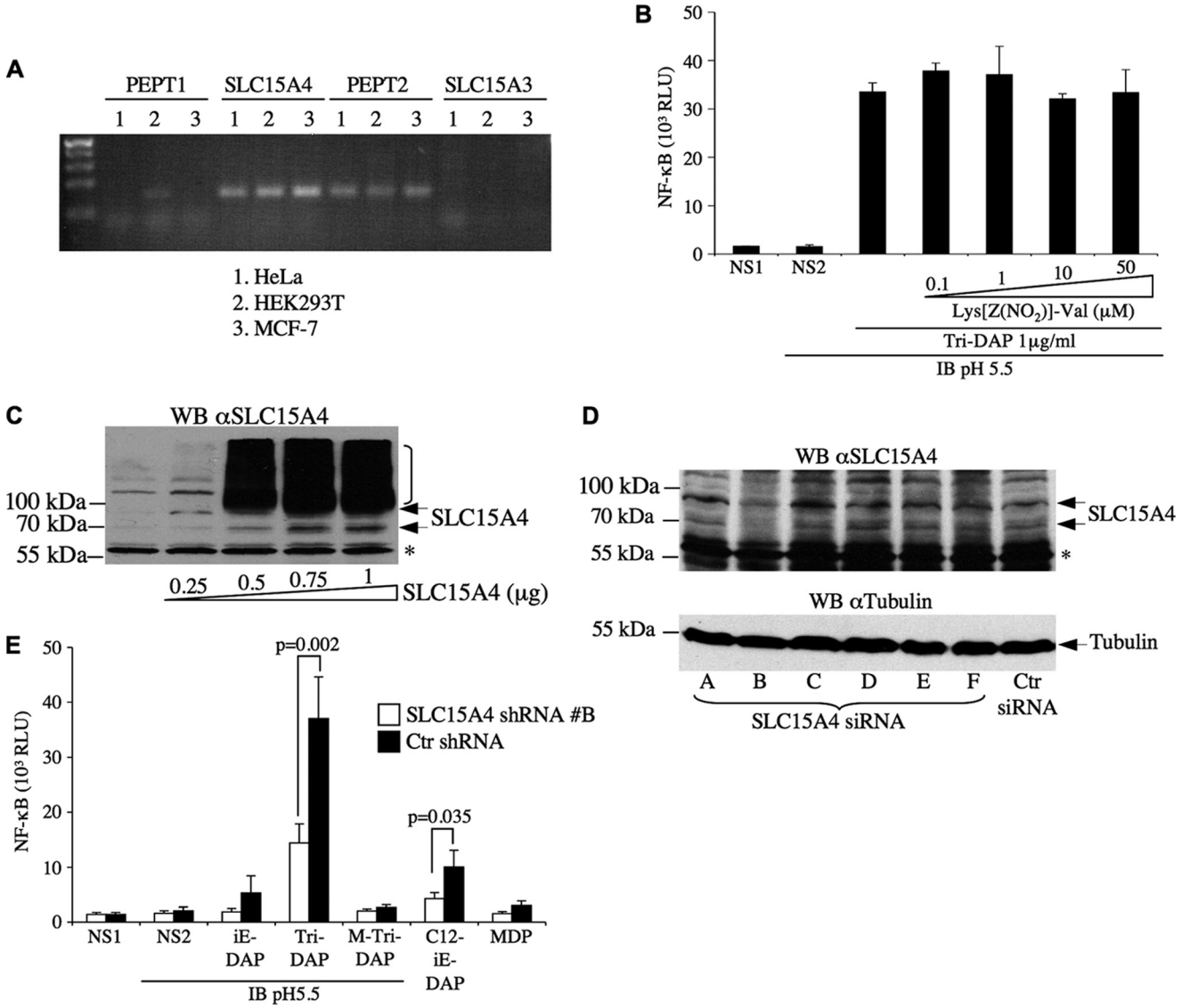

FIGURE 6. **SLC15A4 is involved in Nod1 ligand-mediated NF-κB activation in HEK293T cells.** *A*, the expression of SLC15 proteins was determined by RT-PCR in HeLa, HEK293T, and MCF-7 human epithelial cell lines. *B*, HEK293T cells were transfected overnight with Igκ-luci, and transient acidosis in IB was performed. Cells were stimulated for 1 h with M-Tri-DAP (1 μg/ml) in IB buffer, pH 5.5, in the presence or absence of increasing concentration of the SLC15A2 inhibitor Lys[Z(NO_2)]-Val. *C*, HEK293T cells were transfected with increasing concentrations of SLC15A4-V5 expression vector, and cell lysates were analyzed by Western blotting using anti-SLC15A4 antibody. *, indicates a nonspecific band. *D*, HEK293T cells were transfected for 72 h with various siRNA duplexes (constructs *A–F*) against human SLC15A4 or a control non-targeting siRNA duplex (*Ctr siRNA*) and cell lysates analyzed by Western blotting using anti-SLC15A4 antibody. *, indicates a nonspecific band. The membrane was stripped and blotted against tubulin for loading control. *E*, HEK293T cells transduced for 72 h with lentiviral particles expressing shRNAs against SLC15A4 or a non-targeting sequence were transfected overnight with Igκ-luci and stimulated for 1 h with Nod1 ligands (iE-DAP, Tri-DAP, and M-Tri-DAP) or Nod2 ligand MDP in acidosis conditions (IB, pH 5.5), or with C12-iE-DAP normal (non-acidified) conditions, and luciferase activity was measured 6 h post-stimulation in cell lysates. Statistical analysis was performed using a two-tailed unpaired *t* test, and conditions for which $p < 0.05$ were IB, pH 5.5/Tri-DAP ($p = 0.002$) and C12-iE-DAP ($p = 0.035$). *NS1*, non-stimulated; *NS2*, non-stimulated in IB, pH 5.5.

for the sterically gated internalization of Nod1 ligands to the cytosol. Out of the 46 families of solute carrier (SLC) proteins, only SLC15 proteins are known to transport di- or tri-peptides. Moreover, SLC15 proteins co-transport oligopeptides together with H^+ and have an optimal pH for transport around pH 5.5–6 (33). Therefore, we reasoned that the putative transporter for Nod1 ligands in HEK293T cells might be a member of the SLC15 family. We first analyzed the expression of SLC15 family members in HeLa, HEK293T, and MCF-7 human epithelial cell lines by semi-quantitative PCR. The SLC15 family is composed of four members SLC15A1 to SLC15A4 in mammals. SLC15A3 was not detected in these samples and SLC15A1 was expressed at low levels in HEK293T cells but not HeLa or MCF-7 (Fig. 6*A*). In contrast, transcripts for SLC15A2 and SLC15A4 were strongly expressed in the three cell lines tested (Fig. 6*A*). We first investigated the potential role of SLC15A2 in mediating the transport of Nod1 ligands by using Lys[Z(NO_2)]-Val, a highly specific inhibitor of this transporter ($K_i = 0.097$ μM) (34). Even at the highest non-cytotoxic dose tested (50 μM), the inhibitor failed to inhibit Nod1 ligand-mediated NF-κB activation (Fig. 6*B*), therefore suggesting that SLC15A2 was not required in our experimental system. Similarly, cefadroxil, an antibiotic that inhibits both SLC15A1 and SLC15A2 (34), had no effect on Nod1 ligand-mediated

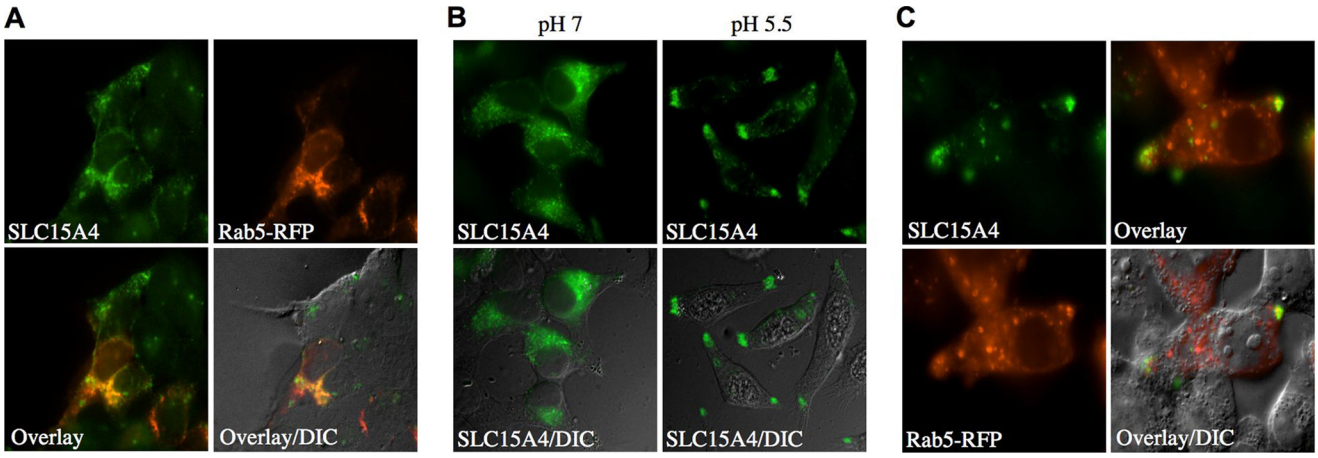

FIGURE 7. **SLC15A4 is expressed in early endosomes.** *A*, HEK293T cells were transfected with SLC15A4-V5 and Rab5-RFP and visualized by immunofluorescence using an anti-V5 antibody. *B*, HEK293T cells were transfected with SLC15A4-V5, cultured for 1 h in IB, pH 7 or pH 5.5, before fixation, and visualized by immunofluorescence using an anti-V5 antibody. *C*, HEK293T cells were transfected with SLC15A4-V5, and Rab5-RFP were cultured for 1 h in IB, pH 5.5, before fixation and visualized by immunofluorescence using an anti-V5 antibody. *Arrows* indicate localization of SLC15A4 and Rab5-RFP at cellular poles.

NF-κB activation (data not shown). We then hypothesized that SLC15A4 could be implicated in the transport of Nod1 ligands. A polyclonal antibody raised against human SLC15A4 revealed multiple forms both at the endogenous level and in SLC15A4-V5-overexpressed cells, migrating at ~60 kDa and higher (Fig. 6*C*), suggesting the existence of extensive post-transcriptional modifications of SLC15A4 in unstimulated conditions. Similar results were obtained using another anti-SLC15A4 polyclonal antibody (data not shown). Next, we tested a number of siRNA constructs designed to knock down endogenous SLC15A4 expression by transient transfection and identified duplex B as the most effective one (Fig. 6*D*), which was used for functional studies. Interestingly, lentiviral-mediated knockdown of SLC15A4 in HEK293T cells resulted in significant decrease of NF-κB activation by the Nod1 ligands Tri-DAP and C12-iE-DAP in luciferase assay (Fig. 6*E*), thus demonstrating that SLC15A4 was critical for Nod1 ligand-mediated signaling in HEK293T cells. In the case of MDP, the results were inconclusive because of the low level of NF-κB activation triggered by this muramyl peptide in our experimental system.

We next investigated the subcellular localization of SLC15A4 by immunofluorescence in HEK293T cells. First, we observed that overexpressed SLC15A4-V5 co-localized with Rab5-RFP, thus showing that this transporter was expressed in early endosomes (Fig. 7*A*). Interestingly, transient extracellular acidosis (pH 5.5), similar to the procedure performed above in luciferase assays, resulted in elongation of the cells and relocalization of SLC15A4 to the cellular poles (Fig. 7*B*), where it partially co-localized with Rab5 (Fig. 7*C*). It is possible that the cellular redistribution of SLC15A4 in early endosomes at mildly acidic pH may contribute to the enhancement of Nod1-dependent signaling that was observed in luciferase assays.

Recent studies have linked IBD to either polymorphisms in genes encoding SLC15 family members (35) or changes in the intestinal expression of SLC15 proteins (36). Because of the implication of *NOD1* and *NOD2* in IBD, we aimed to identify whether the mRNA expression levels of SLC15A4 were altered

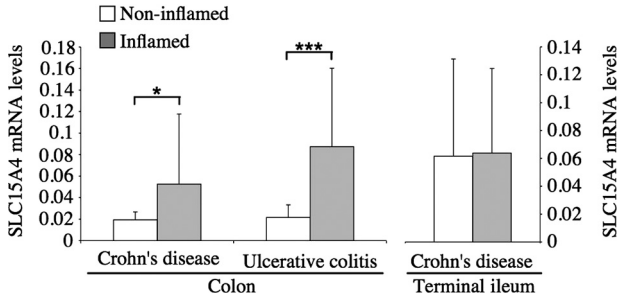

FIGURE 8. **SLC15A4 mRNA expression levels are increased in inflamed colon of IBD patients.** SLC15A4 expression levels in biopsies from colon and terminal ileum of CD and UC patients were determined by absolute quantification of SLC15A4 copy numbers and normalized to mRNA copy numbers of villin. The *bars* represent average values of mRNA expression levels of subgroups of IBD patients. *Error bars* represent S.D. *, $p < 0.05$; ***, $p < 0.0001$.

in the intestine of IBD patients. We analyzed by real-time PCR the expression of SLC15A4 mRNA in colonic biopsies from 53 ulcerative colitis (UC) and 49 Crohn's disease (CD) patients, and inflamed *versus* non-inflamed sections were analyzed separately. For CD patients, inflamed *versus* non-inflamed sections of the terminal ileum were also analyzed. Interestingly, SLC15A4 expression was significantly up-regulated in inflamed areas of the colon in CD ($p < 0.05$) and UC ($p < 0.001$) patients, but not in the terminal ileum of CD patients (Fig. 8).

DISCUSSION

The results that we have presented here establish that, in epithelial cells, muramyl peptides get internalized and traffic via the endocytic machinery, and most likely rely solely on the clathrin-dependent coated pit pathway. This entry pathway is the one generally used for receptor-mediated endocytosis, and this raises the possibility that a cell surface receptor might be involved in the optimal uptake of either muramyl peptides or peptidoglycan-derived di- or tripeptides. In such a scenario, the interaction of these Nod agonists with the cell surface could be either achieved through specific recognition of a peptidic motif by a receptor, or occur non-specifically via electrostatic interactions. It must be noted that our results demonstrated that iE-DAP and Tri-DAP trigger cellular responses in a very differ-

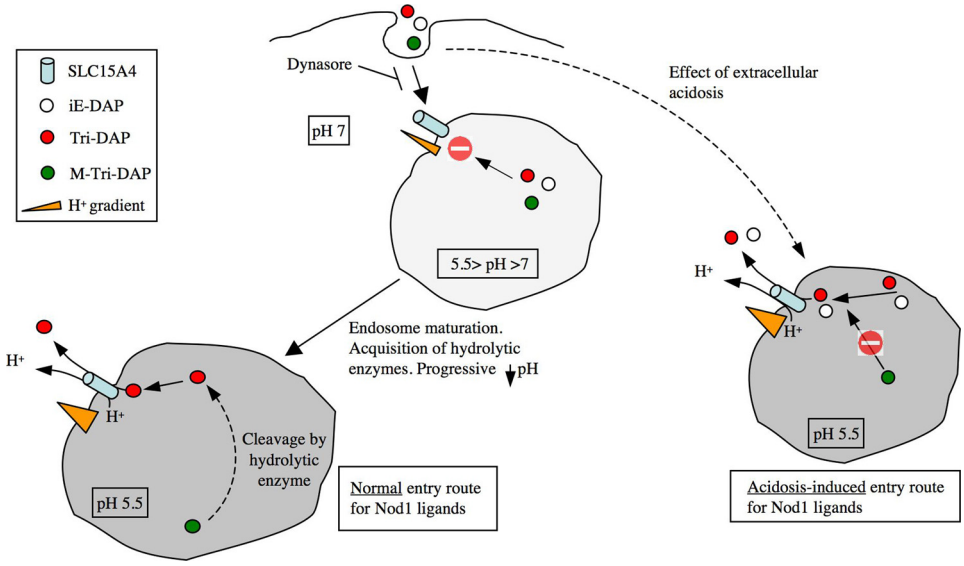

FIGURE 9. **Schematic representation of the model for the entry of Nod1 ligands into epithelial cells.** The normal entry pathway for Nod1 ligands is presented on the *left*, while extracellular acidosis-induced entry is displayed on the *right*. We speculate that acidosis-mediated entry allows bypassing the progressive acidification normally observed in maturing endosomes, resulting in a different vesicular content. In particular, our results suggest that the putative M-Tri-DAP hydrolase, which is normally present in early endosomes, would be absent from experimentally acidified endosomes.

ent fashion, and that this likely results from an inability of iE-DAP to travel down the endocytic pathway to mildly acidified endosomes. It is possible that these observations reflect a differential capacity of these peptides to form interactions with cell surface receptors/proteins, prior to the invagination of the endocytic cup.

Our results showing that Nod ligands are internalized into host cells via endocytosis are consistent with a number of indirect observations of the biological activity of these molecules. In particular, we and others have repeatedly shown that the efficiency of Nod ligands is greatly boosted by "co-transfecting" those ligands overnight together with plasmidic DNA into cationic liposomes (12, 13). Because liposome-DNA complexes are known to traffic mostly via receptor-mediated endocytosis, these initial observations suggested that: (i) the entry of Nod ligands into host cells can be potentiated if these molecules traffic through this pathway and (ii) endocytosis is likely the most critical limiting factor for the stimulating capacities of Nod-activating molecules. In agreement with this, early studies aiming at increasing the stimulating capacities of peptidoglycan-derived peptides or muramyl peptides demonstrated that the covalent addition of lipophilic groups to these structures could greatly enhance cellular responses. For instance, the tumoricidal activity of a lipophilic derivative of MDP on endothelial cells has been found to be enhanced 100- to 1000-fold as compared with MDP (37). Moreover, studies with 6-*O*-acyl derivatives of MDP revealed that 6-*O*-(2-tetradecylhexadecanoyl)-MDP and 6-*O*-(3-hydroxy-2-tetradecyloctadecanoyl)-MDP exhibited stronger macrophage-stimulating effects than MDP (38). Together, a number of convergent studies demonstrated that delivering muramyl peptides via liposomal or fatty acid-containing formulations greatly improved the immunogenicity and adjuvanticity of these bacterial molecules (20–23). Therefore, understanding how Nod ligands enter into cells will help design novel rational strategies aiming at increasing their biological activity. Moreover, it must be noted that in natural conditions, muramyl peptides are rarely found free in the extracellular milieu, and are commonly associated with other bacterial cell wall components that carry fatty acid groups. These include lipoproteins, lipoteichoic acid, mycolic acids, or LPS, and might play a crucial role in the potentiation of endocytosis-mediated entry of Nod ligands.

A recent report has demonstrated that MDP was internalized by macrophages through clathrin-dependent endocytosis (39), which supports our findings in HEK293T cells. However, MDP entry in macrophages appeared to require V-ATPase-dependent endosomal acidification, contrasting with our observations in HEK293T cells. This might be due to differences in the endocytic trafficking machineries of phagocytic *versus* non-phagocytic cells. Alternatively, it is possible that macrophages and epithelial cells rely on different transporters for Nod ligands, which would be expressed in distinct subcellular compartments, such as early endosomes or lysosomes. Indeed, a number of muramyl peptide transporters could exist and be differentially expressed in specific cell types and/or subcellular compartments. This hypothesis is supported by the fact that SLC15A1 was identified as an MDP transporter in Caco-2/bbe epithelial cells (40), but found to be dispensable for mediating MDP entry in macrophages (39). Similarly, SLC15A2 has been shown to trigger transport of the Nod1 ligand iE-DAP in human upper airway epithelial cells (41), but was found to be dispensable in our assays. Finally, it must be noted that the knockdown of SLC15A4 expression in HEK293T cells did not result in a complete ablation of NF-κB activation induced by Nod1 ligands. This suggests that other transporters might contribute to the transport of these peptidoglycan-derived peptides in HEK293T cells and possibly other cell populations.

An interesting question that emerges from our studies is to determine if the limiting factor for Nod-dependent activation is solely the cytosolic presentation of its ligands, or if endocytosis in itself participates in driving NF-κB-dependent activation of Nod1 and Nod2. Indeed, an argument in favor of the latter hypothesis comes from the fact that membrane targeting of Nod2 is required for its ability to trigger NF-κB (42). Moreover, studies on TLR4 argue that the subcellular localization of this protein to early endosomes is required to drive type I interferon responses, through the specific engagement of the adaptor protein TRAM (7). However, our results demonstrate that the sole presentation of Nod ligands to the host cytosol (using the membrane permeabilizing toxin digitonin) is sufficient to recapitulate Nod-dependent activation of NF-κB. This strongly suggests that endocytosis of Nod ligands is

the most efficient means for allowing access of these molecules to the cytosol, but appears dispensable, provided that these molecules could access the cytosol through other means. This observation is of importance, because it implies that Nod proteins could detect free muramyl peptides generated by pathogenic bacteria that would have gained access to the host cytosol, such as *Shigella* or *Listeria*, long after these bacteria would have ruptured the phagosome.

Our results demonstrated that an optimal luminal pH was required for efficient delivery of muramyl peptides into the cytosol, and this correlates with the identification of SLC15A4 as a transporter for Nod1 ligands in early endosomes. Indeed, SLC15 proteins have been shown to display optimal transport properties at mildly acidic pH (ranging from 5.5 to 6) (33). We have also observed that the transport of Nod1 ligands from early endosomes was sterically gated, because iE-DAP and Tri-DAP, but not M-Tri-DAP, were efficiently internalized in our experimental setting of transient acidosis. Again, these results are in agreement with the current knowledge on the steric constraints for SLC15-mediated transport of oligopeptides; indeed, studies on SLC15A1 (43) and SLC15A2 (44) have demonstrated that these transporters have a much greater affinity for di- or tripeptides than other oligopeptides. In this regard, cleavage of the muramyl group by endosomal hydrolytic enzymes such as PGRP-L/PGLYRP2 might represent a prerequisite to SLC15A4-mediated transport of Nod1 ligands to the cytosol. Consequently, we hypothesize that naturally occurring muramyl peptides (such as M-Tri-DAP) are likely processed by endosomal hydrolytic enzymes, which are progressively acquired during normal endosomal maturation (Fig. 9). Therefore, the lack of some critical enzymes from our artificially acidified endosomes likely accounts for the incapacity to process M-Tri-DAP adequately.

Together, our observations characterized the mechanism by which Nod ligands access the host cytosol in human epithelial cells and demonstrated a crucial role for endosomal uptake and pH-dependent transport of these molecules to the cytosol by SLC15A4. Our results provide new avenues for the development of therapeutic strategies aiming at either improving the uptake of muramyl peptides, or targeting the pathway responsible for the cytosolic transport of these bacterial molecules. A better understanding of how Nod proteins detect intracellular bacterial peptidoglycan will provide insights into the etiology of inflammatory diseases such as asthma and CD, which are associated with mutations in *NOD1* and *NOD2*.

Acknowledgments—We thank Dr. Matthias Brandsch (University of Halle, Germany) for providing the SLC15A2-specific inhibitor Lys[Z(NO$_2$)]-Val, Dr. Gregory Knipp (Purdue University) for the kind gift of the SLC15A4 expression plasmid, and Dr. John Brumell (Hospital for Sick Children, Toronto) for the Rab5-RFP expression vector. We also thank Dr. Sergio Grinstein for helpful discussions.

REFERENCES

1. Akira, S., Uematsu, S., and Takeuchi, O. (2006) *Cell* **124,** 783–801
2. Fritz, J. H., Ferrero, R. L., Philpott, D. J., and Girardin, S. E. (2006) *Nat. Immunol.* **7,** 1250–1257
3. Benko, S., Philpott, D. J., and Girardin, S. E. (2008) *Cytokine* **43,** 368–373
4. Akira, S., and Takeda, K. (2004) *Nat. Rev. Immunol.* **4,** 499–511
5. Latz, E., Schoenemeyer, A., Visintin, A., Fitzgerald, K. A., Monks, B. G., Knetter, C. F., Lien, E., Nilsen, N. J., Espevik, T., and Golenbock, D. T. (2004) *Nat. Immunol.* **5,** 190–198
6. Husebye, H., Halaas, Ø., Stenmark, H., Tunheim, G., Sandanger, Ø., Bogen, B., Brech, A., Latz, E., and Espevik, T. (2006) *EMBO J.* **25,** 683–692
7. Kagan, J. C., Su, T., Horng, T., Chow, A., Akira, S., and Medzhitov, R. (2008) *Nat. Immunol.* **9,** 361–368
8. Blander, J. M., and Medzhitov, R. (2004) *Science* **304,** 1014–1018
9. Yates, R. M., and Russell, D. G. (2005) *Immunity* **23,** 409–417
10. Herskovits, A. A., Auerbuch, V., and Portnoy, D. A. (2007) *PLoS Pathog.* **3,** e51
11. Girardin, S. E., Travassos, L. H., Hervé, M., Blanot, D., Boneca, I. G., Philpott, D. J., Sansonetti, P. J., and Mengin-Lecreulx, D. (2003) *J. Biol. Chem.* **278,** 41702–41708
12. Girardin, S. E., Boneca, I. G., Viala, J., Chamaillard, M., Labigne, A., Thomas, G., Philpott, D. J., and Sansonetti, P. J. (2003) *J. Biol. Chem.* **278,** 8869–8872
13. Inohara, N., Ogura, Y., Fontalba, A., Gutierrez, O., Pons, F., Crespo, J., Fukase, K., Inamura, S., Kusumoto, S., Hashimoto, M., Foster, S. J., Moran, A. P., Fernandez-Luna, J. L., and Nuñez, G. (2003) *J. Biol. Chem.* **278,** 5509–5512
14. Chamaillard, M., Hashimoto, M., Horie, Y., Masumoto, J., Qiu, S., Saab, L., Ogura, Y., Kawasaki, A., Fukase, K., Kusumoto, S., Valvano, M. A., Foster, S. J., Mak, T. W., Nuñez, G., and Inohara, N. (2003) *Nat. Immunol.* **4,** 702–707
15. Girardin, S. E., Boneca, I. G., Carneiro, L. A., Antignac, A., Jéhanno, M., Viala, J., Tedin, K., Taha, M. K., Labigne, A., Zähringer, U., Coyle, A. J., DiStefano, P. S., Bertin, J., Sansonetti, P. J., and Philpott, D. J. (2003) *Science* **300,** 1584–1587
16. Magalhaes, J. G., Philpott, D. J., Nahori, M. A., Jéhanno, M., Fritz, J., Bourhis, L., Viala, J., Hugot, J. P., Giovannini, M., Bertin, J., Lepoivre, M., Mengin-Lecreulx, D., Sansonetti, P. J., and Girardin, S. E. (2005) *EMBO Rep.* **6,** 1201–1207
17. Lederer, E. (1980) *J. Med. Chem.* **23,** 819–825
18. Lederer, E. (1986) *Drugs Exp. Clin. Res.* **12,** 429–440
19. Traub, S., Kubasch, N., Morath, S., Kresse, M., Hartung, T., Schmidt, R. R., and Hermann, C. (2004) *J. Biol. Chem.* **279,** 8694–8700
20. Fogler, W. E., and Fidler, I. J. (1987) *Int. J. Immunopharmacol.* **9,** 141-150
21. Mehta, K., Lopez-Berestein, G., Hersh, E. M., and Juliano, R. L. (1982) *J. Reticuloendothel. Soc.* **32,** 155–164
22. Nayar, R., Schroit, A. J., and Fidler, I. J. (1986) *Methods Enzymol.* **132,** 594–603
23. Schroit, A. J., and Fidler, I. J. (1982) *Cancer Res.* **42,** 161–167
24. Le Bourhis, L., Benko, S., and Girardin, S. E. (2007) *Biochem. Soc. Trans.* **35,** 1479–1484
25. Hugot, J. P., Chamaillard, M., Zouali, H., Lesage, S., Cézard, J. P., Belaiche, J., Almer, S., Tysk, C., O'Morain, C. A., Gassull, M., Binder, V., Finkel, Y., Cortot, A., Modigliani, R., Laurent-Puig, P., Gower-Rousseau, C., Macry, J., Colombel, J. F., Sahbatou, M., and Thomas, G. (2001) *Nature* **411,** 599–603
26. Ogura, Y., Bonen, D. K., Inohara, N., Nicolae, D. L., Chen, F. F., Ramos, R., Britton, H., Moran, T., Karaliuskas, R., Duerr, R. H., Achkar, J. P., Brant, S. R., Bayless, T. M., Kirschner, B. S., Hanauer, S. B., Nuñez, G., and Cho, J. H. (2001) *Nature* **411,** 603–606
27. Macia, E., Ehrlich, M., Massol, R., Boucrot, E., Brunner, C., and Kirchhausen, T. (2006) *Dev. Cell* **10,** 839–850
28. Drubin, D. G., Kaksonen, M., Toret, C., and Sun, Y. (2005) *Novartis Found. Symp.* **269,** 35–42; discussion 43–36, 223–230
29. Kaksonen, M., Toret, C. P., and Drubin, D. G. (2006) *Nat. Rev. Mol. Cell Biol.* **7,** 404–414
30. Steinberg, B. E., Huynh, K. K., and Grinstein, S. (2007) *Biochem. Soc. Trans.* **35,** 1083–1087
31. Gutierrez, O., Pipaon, C., Inohara, N., Fontalba, A., Ogura, Y., Prosper, F., Nunez, G., and Fernandez-Luna, J. L. (2002) *J. Biol. Chem.* **277,** 41701–41705
32. Rosenstiel, P., Fantini, M., Bräutigam, K., Kühbacher, T., Waetzig, G. H.,

Seegert, D., and Schreiber, S. (2003) *Gastroenterology* **124,** 1001–1009
33. Daniel, H., and Kottra, G. (2004) *Pflugers Arch.* **447,** 610–618
34. Biegel, A., Knütter, I., Hartrodt, B., Gebauer, S., Theis, S., Luckner, P., Kottra, G., Rastetter, M., Zebisch, K., Thondorf, I., Daniel, H., Neubert, K., and Brandsch, M. (2006) *Amino Acids* **31,** 137–156
35. Zucchelli, M., Torkvist, L., Bresso, F., Halfvarson, J., Hellquist, A., Anedda, F., Assadi, G., Lindgren, G. B., Svanfeldt, M., Janson, M., Noble, C. L., Pettersson, S., Lappalainen, M., Paavola-Sakki, P., Halme, L., Farkkila, M., Turunen, U., Satsangi, J., Kontula, K., Lofberg, R., Kere, J., and D'Amato, M. (2009) *Inflamm. Bowel Dis.*
36. Wojtal, K. A., Eloranta, J. J., Hruz, P., Gutmann, H., Drewe, J., Beglinger, C., Fried, M., Kullak-Ublick, G. A., and Vavricka, S. R. (2009) *Drug Metab. Dispos.*
37. Phillips, N. C., Stewart-Phillips, J., and Wang, P. (1994) *J. Immunother Emphasis Tumor Immunol.* **15,** 185–193
38. Takada, H., Tsujimoto, M., Kato, K., Kotani, S., Kusumoto, S., Inage, M., Shiba, T., Yano, I., Kawata, S., and Yokogawa, K. (1979) *Infect Immun.* **25,** 48–53
39. Marina-García, N., Franchi, L., Kim, Y. G., Hu, Y., Smith, D. E., Boons, G. J., and Núñez, G. (2009) *J. Immunol.* **182,** 4321–4327
40. Vavricka, S. R., Musch, M. W., Chang, J. E., Nakagawa, Y., Phanvijhitsiri, K., Waypa, T. S., Merlin, D., Schneewind, O., and Chang, E. B. (2004) *Gastroenterology* **127,** 1401–1409
41. Swaan, P. W., Bensman, T., Bahadduri, P. M., Hall, M. W., Sarkar, A., Bao, S., Khantwal, C. M., Ekins, S., and Knoell, D. L. (2008) *Am. J. Respir. Cell Mol. Biol.* **39,** 536–542
42. Barnich, N., Aguirre, J. E., Reinecker, H. C., Xavier, R., and Podolsky, D. K. (2005) *J. Cell Biol.* **170,** 21–26
43. Fei, Y. J., Kanai, Y., Nussberger, S., Ganapathy, V., Leibach, F. H., Romero, M. F., Singh, S. K., Boron, W. F., and Hediger, M. A. (1994) *Nature* **368,** 563–566
44. Boll, M., Herget, M., Wagener, M., Weber, W. M., Markovich, D., Biber, J., Clauss, W., Murer, H., and Daniel, H. (1996) *Proc. Natl. Acad. Sci. U.S.A.* **93,** 284–289